5-2016

Acoustic firearm discharge detection and classification in an enclosed environment

Lorenzo Luzi

Eric Gonzalez

Paul Bruillard

Matthew Prowant

James Skorpik

See next page for additional authors

Acoustic firearm discharge detection and classification in an enclosed environment

Lorenzo Luzi,[1] Eric Gonzalez,[1] Paul Bruillard,[1] Matthew Prowant,[1] James Skorpik,[1] Michael Hughes,[1,a)] Scott Child,[2] Duane Kist,[2] and John E. McCarthy[3]
[1]*Pacific Northwest National Laboratory, Richland, Washington 99354, USA*
[2]*Kennewick Police Department SWAT Team, 211 West 6th Avenue, Kennewick, Washington 99336-0108, USA*
[3]*Department of Mathematics, Washington University in Saint Louis, Campus Box 1146, St. Louis, Missouri 63130, USA*

(Received 19 October 2015; revised 19 April 2016; accepted 26 April 2016; published online 13 May 2016)

Two different signal processing algorithms are described for detection and classification of acoustic signals generated by firearm discharges in small enclosed spaces. The first is based on the logarithm of the signal energy. The second is a joint entropy. The current study indicates that a system using both signal energy and joint entropy would be able to both detect weapon discharges and classify weapon type, in small spaces, with high statistical certainty. [http://dx.doi.org/10.1121/1.4948994]

[MRB] Pages: 2723–2731

I. INTRODUCTION

We report on methods to both detect and classify firearm discharges in small, enclosed, environments with high statistical certainty. Some algorithms reported on here are capable of running on an embedded microcontroller system (Texas Instruments FRAM micro-controller unit number MSP430FR5989) that, with an associated microphone (InvenSense INMP404ACEZ-R7 microphone), is capable of signal acquisition and analysis. Moreover, such a system and software are suitable for wide-scale deployment in classrooms, movie theaters, and other public gathering places.

Implementation on a microcontroller limits the sophistication of algorithms that may be employed. In addition, we have found that the governing dynamics of acoustic propagation and signal acquisition are highly nonlinear. Consequently, we have focused on approaches that reduce a waveform, or a subsegment of a waveform $f(t)$, to a single number. This number, or receiver value, is then intended to be used as the basis for signal identification. Signal energy, or its logarithm, denoted $\log[E_f]$, combined with careful signal filtering has been shown to provide a good balance between computational complexity and statistical sensitivity. Our results show that signal energy analysis is able to clearly discriminate between firearm discharges and other acoustic background events, but not necessarily between firearm types.

This information is a critical factor in determining first responder tactics and strategy. To address the need to identify weapon types from their acoustic signatures, we have investigated various entropies as previous studies have demonstrated their utility for analysis of ultrasonic signals in both materials characterization and medical ultrasonics.[1–13] The current study demonstrates the utility of entropies for analysis of acoustic signals in the audio range as well. When used in conjunction with energy analysis it appears that acoustic discrimination of weapon type is also possible.

There is an extensive literature on firearm discharge detection and source identification. Previous investigations of firearm discharge have focused on outdoor source location,[14–16] and identification of firearm and ammunition type using shockwave analysis.[17,18] Other investigators have studied correlation and linear predictive coding for firearm detection and source recognition.[19] Threshold detection schemes using six different waveform characteristics, e.g., magnitude of signal absolute value, median filter, Teager energy operator, correlation against a template, among others mainly for outdoor gunshot detection and source classification have been described by Chacón-Rodríguez *et al.*[20] More generally, extraction of acoustic cues for forensic purposes has been investigated by Hong and colleagues.[21]

The current study is different from prior work in that it considers signals acquired indoors, in relatively small enclosures. Moreover, shockwave analysis or linear analysis techniques for source identification are not used at all.

II. DATA ACQUISITION

Two different groups of acoustic data were collected for this study. This first group consisted of "threat-type" signals, which were acquired by discharging several different firearms into a ballistic trap: 223 caliber automatic rifle [M-16 assault rifle (Colt's Manufacturing Company, LLC, Hartford, CT); Fiocchi 45 grain frangible (Fiocchi of America, Inc., Ozark, MO)]. 40 caliber semi-automatic pistol [Compact Smith & Wesson (Smith & Wesson, Springfield, MA); S&W 125 grain frangible], 45 caliber automatic pistol [Taurus PT 145 PRO (Taurus Inc, Miami Lakes, FL); Fiocchi 155 grain frangible], 9 mm semi-automatic pistol [Springfield Armory (Springfield Armory® Geneseo, IL) XD9; Fiocchi 100 grain luger], 22 rifle [Marlin model 60 (Marlin Firearms, subsidiary of Freedom Group Madison, North Carolina); Remington 22LR 40 grain], 22 pistol [Intratec TEC-22 (Intratec Firearms, Miami, FL); Remington (Remington Arms Company, LLC, Madison, NC) 22LR 40 grain], 357 magnum (S&W Magnum; PMC

a)Electronic mail: michael.s.hughes@pnnl.gov

158 grain), 380 caliber pistol [Taurus (Taurus International Manufacturing, Miami Lakes, FL) PT 738; Fiocchi 380 auto], 38 special (S&W.38 Special AirLite; American Eagle 158 grain), and AK 47 [SAIGA 7.62×39 Legion (Kalashnikov Concern, Izhevsk, Russia); Tula 7.62×39 R 124 HP]. All firearms but the M16 where provided by the Kennewick, WA police department from their evidence locker, the M16 was provided by their special weapons and tactics team. This was done in order to sample an ensemble of acoustic sources that captures the variability found in non military/police arms, i.e., in "street" weapons. A second group of control data was also acquired. These consisted of "false" alarms: a book slapped on a table, an air-filled paper bag "popping," and a wrench striking a metal ladder.

Signals were collected in three different rooms of different dimensions: a large auditorium (12.8×8.4 m; height 2.7 m), a medium sized meeting room (4.6×6.1 m; height 2.7 m), and a small office (3.7×3.7 m; height 2.7 m). Acquisition of all data were completed during one 10 h interval. Firearm discharge data were obtained with the assistance of the Kennewick, WA special weapons and tactics team, whose members volunteered to operate all firearms used in this study. We will report on results collected in the small room shown in Fig. 1 since this constitutes the most challenging environment in which to distinguish between threat and nonthreat acoustic events and to discriminate between different types of threats. The figure shows the dimensions of the room, the placement of the microphones, location of trap, and firearms operator. During acquisition of data, the door to the room was closed.

Acoustic signals were converted to electrical signals using a InvenSense INMP404ACEZ-R7 microphone connected to custom built amplifier circuitry. These signals were digitized, single-shot fashion, by a Teledyne LeCroy MSO $104MX_s$ B digital sampling oscilloscope to obtain raw data consisting of one million point waveforms (12-bit numbers; 1.0 MHz sampling rate). At least five waveforms for each type of acoustic source were acquired and stored for later analysis.

III. ANALYSIS

A. Experimental nonlinearities

Several observations indicate that the experiment is governed, at least partially, by nonlinear dynamics occurring during the propagation of sound as well in the microphone during data capture. During acquisition of firearms signals, the marksman reported the ceiling tile immediately above the trap was being visibly displaced by the weapon discharge. Subsequent inspection of the digital waveforms on a fine time scale (not shown) reveals evidence of shock-like features. Moreover, the amplitude of firearm discharges in typically in over 100 dB and this is close to the rated limit of the microphone used in our study.

As an initial test of this hypothesis, we acquired waveforms for a single- and five-round discharge from the 223 caliber assault rifle. Figure 2 shows, in its top panel, the waveform recorded from the discharge of one round, $f_1(t)$. The waveform, $f_5(t)$, for five automatic discharges is shown in the middle panel. Both waveforms were Fourier

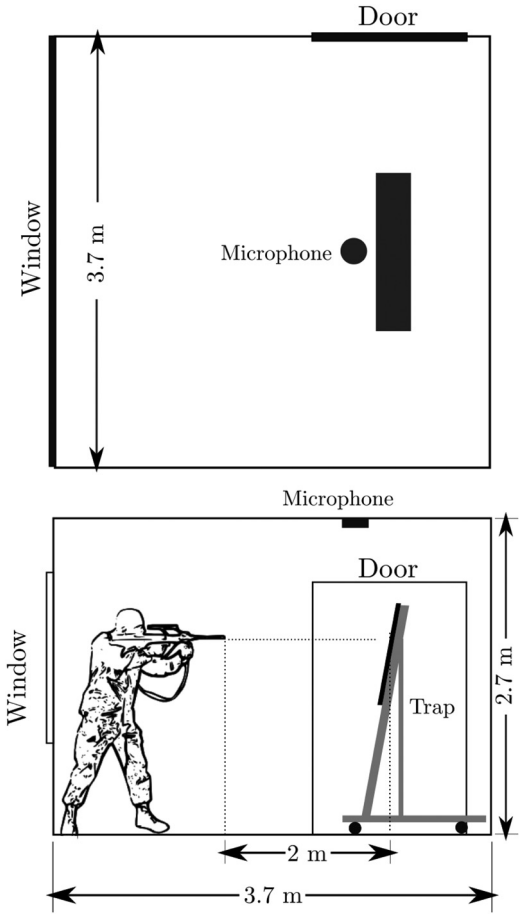

FIG. 1. Geometry used for acoustic signal acquisition.

transformed to obtain, respectively, $F_1(\omega)$ and $F_5(\omega)$. If the propagation was linear, or even weakly linear, then the inverse Fourier transform of $F_5(\omega)/F_1(\omega)$ should produce a time series having five delta function spikes. To avoid division by zero we actually divide by a modified version of $F_1(\omega)$, specifically

$$\frac{F_5(\omega)}{\tilde{F}_1(\omega)}, \tag{1}$$

where

$$\tilde{F}_1(\omega) = \begin{cases} F_1(\omega) & \text{if } |F_1(\omega)| \geq \rho, \\ \rho & \text{if } |F_1(\omega)| < \rho, \end{cases} \tag{2}$$

and $\rho = 10^{-6}$ is a regularizing term. The inverse Fourier transform of this function was computed and is shown in the bottom panel of the Fig. 2. It is evident that there is no pulse train.

The strong nonlinearities exhibited by the acoustics preclude identification of signal source using signal processing techniques based on linear systems theory such as matched filters. Instead, we will focus on techniques that take subsegments of the acoustic waveform and produce a single number or receiver value. Moreover, repeated monitoring of microphone performance was undertaken during and after the acquisition of firearm discharge waveforms to detect signs of damage resulting from exposure to large amplitude sound waves. These are reported on more fully in the Appendix.

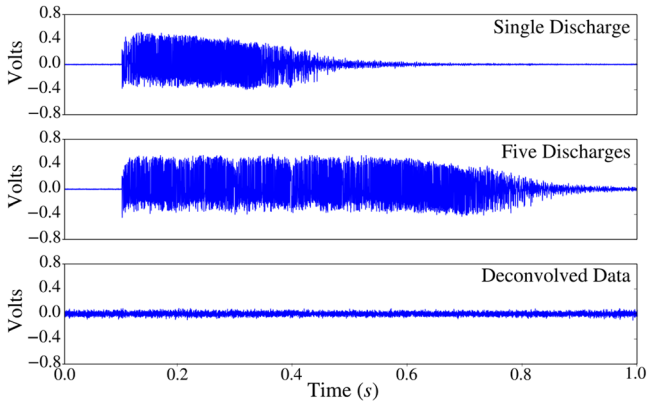

FIG. 2. (Color online) Top panel: Acoustic signature of one discharge of 223 caliber assault rifle. Middle panel: acoustic signature of automatic discharge of five rounds. Bottom panel: The deconvolution, as discussed in connection with Eqs. (1) and (2) below, of the five discharge by the single discharge signature. In a linear system such a deconvolution should produce a series of five delta functions. The fact that these are not evident supports the conclusion that acoustic wave propagation is not linear in the current study.

B. Energy and entropy analysis of waveforms

We will denote the acoustic waveforms acquired for our study by $f(t)$. We will also employ the convention that the domain of $f(t)$ is [0, 1].

For $f(t)$, the signal energy is

$$E_f = \int_0^1 f(t)^2 dt. \tag{3}$$

We may also compute a joint entropy of acoustic waveforms, $f(t)$, using a reference function $g(t)$. In the case where $f(t)$ and $g(t)$ are differentiable functions this entropy is given by[6]

$$H_{f,g} \equiv -\frac{1}{2}\int_0^1 dt \frac{\min\left[|f'(t)|, |g'(t)|\right]}{\max\left[|f'(t)|, |g'(t)|\right]} - \int_0^1 dt \log\left\{\max\left[|f'(t)|, |g'(t)|\right]\right\}. \tag{4}$$

The strategy for choosing the reference waveform, $g(t)$, in the case where subtle changes in $f(t)$ must be detected has been described elsewhere.[7] Although these techniques are not technically applicable for the present investigation, we will take them as an operational starting point. The justification for this approach is twofold. In previous studies,[8,9] it has been observed that the joint entropy calculation has many of the attributes of a matched filter. In particular, $H_{f,g}$ is often extremized for waveforms "close" to $f(t)$, when $g'(t)$ is a step-like function, with transitions located at the critical values of $f(t)$. In addition, Theorem 1 of a previous study of the variational properties of joint entropy[7] also suggests that this strategy would be successful. Consequently, we will use this approach, described in greater detail below (Fig. 4) to discriminate between different classes of firearms.

C. Signal preprocessing

The goal of this study was to discover a suite of signal receivers that are suitable for two different tasks: discharge detection vs firearm identification. Consequently, after an initial "gating" operation to remove the noise-only pre-trigger portion of the digital waveform, two different preprocessing schemes were applied to the raw data, prior to computation of either signal energy or entropy.

For signal energy computations the data were decimated (i.e., only every tenth point was kept) and then bandpass filtered to exclude frequencies outside of the range extending from 1 to 26 kHz. This was accomplished in the frequency domain by multiplying the Fourier transform of the raw data by the conjugate symmetric form of

$$\frac{\left[\tanh\left(\frac{f-f_{l.b.}}{a}\right)+1\right]\left[\tanh\left(\frac{f_{u.b.}-f)}{a}\right)+1\right]}{4}, \tag{5}$$

where $f_{l.b.} = 10^3$, $f_{u.b.} = 26 \times 10^3$, and the sharpness parameter for the filter was set to $a = 10$. All computations are performed using units of Hertz.

The logarithm of the signal energy was computed, according to Eq. (3) using 2.56 ms segments of the acoustic waveforms. The analysis was performed using a "moving window" analysis where the 2.56 ms window was placed initially at a point coincident with the signal arrival and the logarithm of the signal energy was computed. Subsequently, the window was moved in 2.56 ms steps, until the end of the data were reached. In this way, an array of signal energy log values was produced. In this study it was observed that analysis with the window placed at zero time was adequate for source classification.

For entropy calculations only 32 μs segments of the acoustic waveforms were analyzed in moving window fashion, with a moving window shift of 1 μs. The rationale for the shorter window length was that its structure would be primarily determined by the attributes of the firearm and not those of the environment. As in the signal energy case, it was found that analysis with the window placed at zero time was adequate for source classification. This observation and sensitivity to placement and length of the moving window will be more fully explained below in connection with Fig. 6.

IV. RESULTS

A. "Threat" vs "nonthreat"

Each of the waveforms acquired for each source type were analyzed as described above to obtain either log energy, $\log[E_f]$, or joint entropy, $H_{f,g}$. The mean and standard deviations of the ensemble for each source were then computed.

Figure 3 shows the results obtained for the $\log[E_f]$ analysis. The error bars in the plot are equal to one standard deviation. There is wide separation between the threat-type and nonthreat-type bars. However, there appears to be little separation between either the 223 caliber (M16) and AK47 ("long rifles") and any pistols. This would be useful information in certain circumstances.

In order to quantify this separation, the pair-wise differences between each acoustic source were computed along with associated standard deviation using the standard

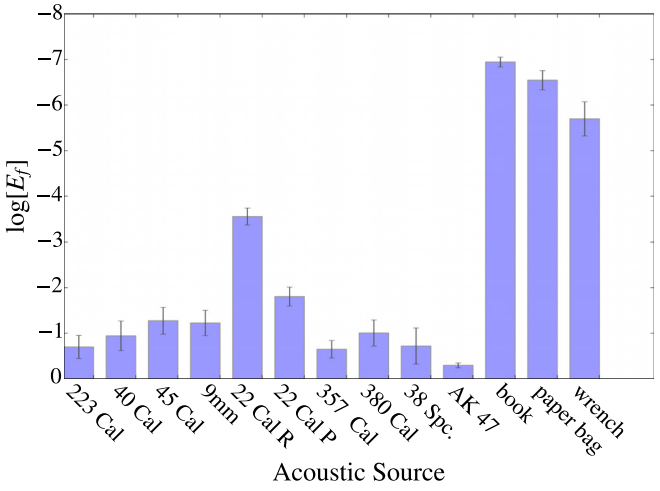

FIG. 3. (Color online) Separation of "threat-type" vs "nonthreat-type" by the logarithm of signal energy, log[E_f].

methods for error propagation.[22] From these, the mean difference, which can be either positive or negative, divided by the associated standard deviation was computed in order to obtain a noise-normalized measure of change between receiver values for different acoustic sources. This ratio, which we will use to quantify the sensitivity of analysis techniques, is often defined as the statistical confidence,[23] and is the reciprocal of the coefficient of variation of a random variable. Larger values are better as they imply greater statistical separation between random variables, in our case signal receivers. Small values suggest that the sources are statistically indistinguishable to the signal receiver.

The confidence values characterizing the relation between threat-type and nonthreat-type-signals are summarized in Table I. We observe that all confidences are larger than one, suggesting that these types of signals should be easily distinguished using only log[E_f]. Moreover, energy calculation is simple and well suited to our goal of reduction-to-practice on low cost hardware.

B. Threat-type discrimination

As mentioned previously, discrimination between threat-type waveforms would be useful information. Table II summarizes the absolute values of all confidence ratios obtained in pair-wise comparison of log[E_f] values for threat-type sources. Only the values below the diagonal are shown since the table is symmetric about this line. We observe that many entries are greater than one, suggesting that in many cases highly reliable discrimination between sources is possible. However, there are also many entries that are less than one. Particularly troubling is the fact that several of these entries appear in the first column indicating that log[E_f] provides poor discrimination between several pistols and the assault rifle.

TABLE I. Confidence ratios of "threat-type" vs "nonthreat-type" sources using log[E_f].

	Book	Paper bag	Wrench
223 cal. semiauto rifle	22.60	17.68	11.03
40 cal. semiauto pistol	17.50	14.43	9.57
45 cal. semiauto pistol	18.10	14.5	9.28
9 mm semiauto pistol	19.22	15.26	9.59
22 cal. semiauto rifle	15.81	10.63	5.11
22 cal. semiauto pistol	22.07	16.05	9.09
357 cal. revolver pistol	28.66	20.69	12.00
380 cal. semi auto pistol	19.41	15.57	9.95
38 special revolver pistol	15.19	13.00	9.13
AK47 semiauto rifle	55.76	28.77	14.28

Consequently, we have investigated the use of different joint entropies, H_{f,g_i}, as an additional tool for weapons identification. Each reference function, $g_i(t)$, was generated using one of the threat-type waveforms according to the methods described previously,[7] for instance $g_1(t)$ was computed using one of the 223 rile waveforms, $g_2(t)$ was computed using one of the 40 caliber waveforms and so forth with $g_{10}(t)$ being computed using one of the AK47 rifle waveforms. For completeness, we illustrate this computation in Fig. 4. The line with long and short dashes shows the a portion of the bandpass filtered version of the underlying waveform coincident with the onset of the acoustic pulse generated by discharge of the 223 assault rifle. Zero time indicates the point at which the LeCroy MSO 104MX$_s$ B digital sampling oscilloscope triggered during data acquisition when the incoming voltage crossed the threshold level of roughly 125 mV. The 32 μs segment of this waveform, which has been selected for H_{f,g_i} analysis is shown by the solid line. Solid black circles indicate the locations of the start of this segment and its extrema. The dashed step-like function shows a scaled version of the resulting $g_1'(t)$, which had high values of 10 000 and low values of 0.001.

An example plot of the entropies H_{f,g_1}, along with associated standard deviation bars, obtained using the reference function generated using a 223 caliber waveform is shown in Fig. 5. The figure shows a clear separation between the "long rifle" 223 data and the "pistol" 40 caliber, 45 caliber, and to a lesser extent, 9 mm data. For this plot, the confidence ratios quantifying the separation between the 223 (a "long rifle") and the 357 caliber and 380 caliber pistols data improves from the Table II values of 0.16 and 0.80 to 5.58 and 5.69, respectively. However, for the 22 caliber rifle to confidence is decreased from its Table II value of 9.09 to 5.64.

To be thorough, we have calculated confidence tables for joint entropy analogous to the Table II using a representative of each type of "threat" waveform, i.e., for all $g_i(t), i = 1, \ldots, 10$. To assess the sensitivities obtainable using this suite of signal receivers, the maximum absolute values for each entry in these over all 10 tables have been collected and are shown in Table III. We observe that where the entries of this table are low, the corresponding entries of Table II are high and vice versa. Moreover, the maximum always exceeds one.

C. Effect of changing analysis parameters, particularly moving window placement

We have explored other values for bandpass filter lower and upper bound, moving window length, moving window

TABLE II. Confidence ratios for different "threat-type" sources obtained using $\log[E_f]$ analysis.

	223	40 Cal.	45 Cal.	9 mm	22 Cal (R)	22 Cal (P)	357 Cal	380 Cal	38 Spc.	AK 47
223 cal. semiauto rifle (M16)	-	-	-	-	-	-	-	-	-	-
40 cal. semiauto pistol	0.59	-	-	-	-	-	-	-	-	-
45 cal. semiauto pistol	1.48	0.76	-	-	-	-	-	-	-	-
9 mm semiauto pistol	1.40	0.66	0.12	-	-	-	-	-	-	-
22 cal. semiauto rifle	9.09	6.98	6.57	7.00	-	-	-	-	-	-
22 cal. semiauto pistol	3.37	2.23	1.47	1.67	6.32	-	-	-	-	-
357 cal. revolver pistol	0.16	0.78	1.78	1.71	10.92	4.10	-	-	-	-
380 cal. semiauto pistol	0.80	0.14	0.66	0.55	7.49	2.26	1.03	-	-	-
38 special revolver pistol	0.04	0.44	1.13	1.05	6.50	2.43	0.16	0.58	-	-
AK47 semiauto rifle	1.55	1.96	3.28	3.29	16.96	7.07	1.77	2.43	1.06	-

step in the course of our investigations. The choice of band-pass filter parameters is largely governed by the response characteristics of microphone and where chosen primarily to eliminate electronic noise outside of the spectral response of that device. However, the choice of moving window parameters appears to be less constrained and during the course of our investigations the impact of varying these over a range of values was explored. For signal energy analysis it was found that windows containing at least half of the waveforms were suitable for classification. However, entropy analysis appears to be more tightly constrained, particularly in connection with the, more difficult, problem of classification of weapon type. Consequently, we now present additional information of the choice of values reported.

Our primary criterion for utility was that these parameters cover a continuous range of values. We have found that for window length the values reported above may be more than doubled before entropy analysis is unable to distinguish weapon types. While moving window position, which was computed for an array of values, and should be chosen to capture physical events is not sensibly characterized this way, we have found that it may be chosen in an interval that is long enough to be easily captured by current digital acquisition devices. We focus on the comparison of 223 assault rifle and 40 caliber pistol in the discussion that follows as it is a typical result. The sensitivity of $H_{f,g}$ analysis to this parameter is illustrated in three panels shown in Fig. 6, where the analysis of a waveform captured from discharge of the 223 caliber assault rifle is compared with a discharge from a 40 caliber pistol. In the top panel are shown 110 μs segments that capture the arrival of the acoustic waveforms at the sensor. We observe that the shape of the pulses at first arrival is noticeably different. This observation motivated the entropy analysis investigation, which previous reports have shown is more sensitive to changes in shape of waveforms than is signal energy analysis.[24] The middle panel shows the curves for processed raw data (as described in Sec. III C) overlain with circular symbols placed at the locations of the 32 time domain points used to compute $H_{f,g}$ incorporated into Fig. 5). Also shown in the middle panel is a gray region containing twenty points that were also used as the starting points for 32 μ windows over which $H_{f,g}$ was computed as part of the moving window analysis as described in Sec. III C. The bottom panel shows the resulting $H_{f,g}$ for both firearms. Only the first four and the last three points, where the error bars of the firearms overlap, fail to distinguish the two weapon types. These results, which are also typical of signal energy, show that the reported $H_{f,g}$ results summarized in Fig. 5 are, at least to the order of a

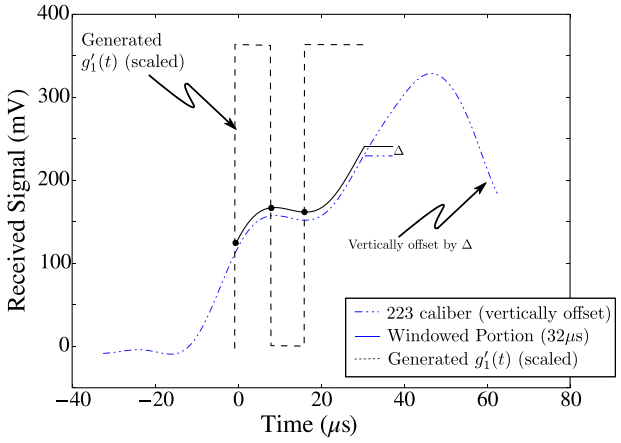

FIG. 4. (Color online) An illustration of the steps used to calculate a reference waveform for the 223 caliber assault rifle. The dashed step-like function is the derivative of the calculated reference function $g_1'(t)$, which is shown instead of the reference $g_1(t)$, since its relation to the extrema of 32 μs segment is more easily visualized.

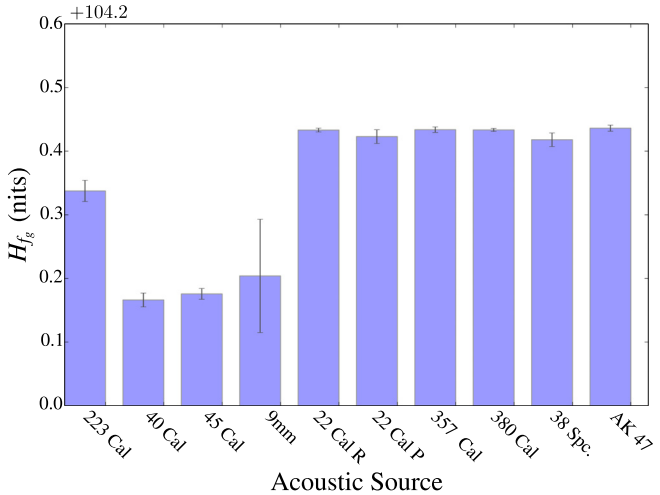

FIG. 5. (Color online) Separation of the acoustic signatures of different firearms by joint entropy, $H_{f,g}$. The reference was computed using a step-like function with transitions at the extrema of one of the 223 assault rifle waveforms. Note vertical axis constant offset of 104.2.

TABLE III. Maximum confidence ratios for different "threat-type" sources obtained using $H_{f,g}$ analysis for $g_i(t)$ derived from different acoustic sources as described in Sec. IV B.

	223	40 Cal.	45 Cal.	9 mm	22 Cal. (R)	22 Cal. (P)	357 Cal	380 Cal	38 Spc.	AK 47
223 cal. rifle semiauto rifle(M16)	-	-	-	-	-	-	-	-	-	-
40 cal. semiauto pistol	8.61	-	-	-	-	-	-	-	-	-
45 cal. semiauto pistol	8.63	1.42	-	-	-	-	-	-	-	-
9 mm semiauto pistol	1.48	1.00	0.65	-	-	-	-	-	-	-
22 cal. semiauto rifle	5.64	53.46	29.92	7.40	-	-	-	-	-	-
22 cal. semiauto pistol	4.30	38.33	18.00	9.33	1.16	-	-	-	-	-
357 cal. revolver pistol	5.58	40.44	27.67	9.71	0.91	1.74	-	-	-	-
380 cal. semiauto pistol	5.69	59.04	31.65	9.80	1.24	1.94	0.58	-	-	-
38 special revolver pistol	4.06	16.59	17.75	6.01	1.37	0.48	1.37	1.42	-	-
AK47 semiauto rifle	5.67	37.20	26.57	9.79	0.95	1.96	0.49	0.51	1.55	-

few microseconds, insensitive to analysis window placement as long as it primarily encompasses the arrival of the waveform. Given the capabilities of modern data acquisition equipment in relation to the length of this window of stability, it seems reasonable to conclude that $H_{f,g}$ can provide a robust metric for classifying acoustic signatures into different weapon-type categories.

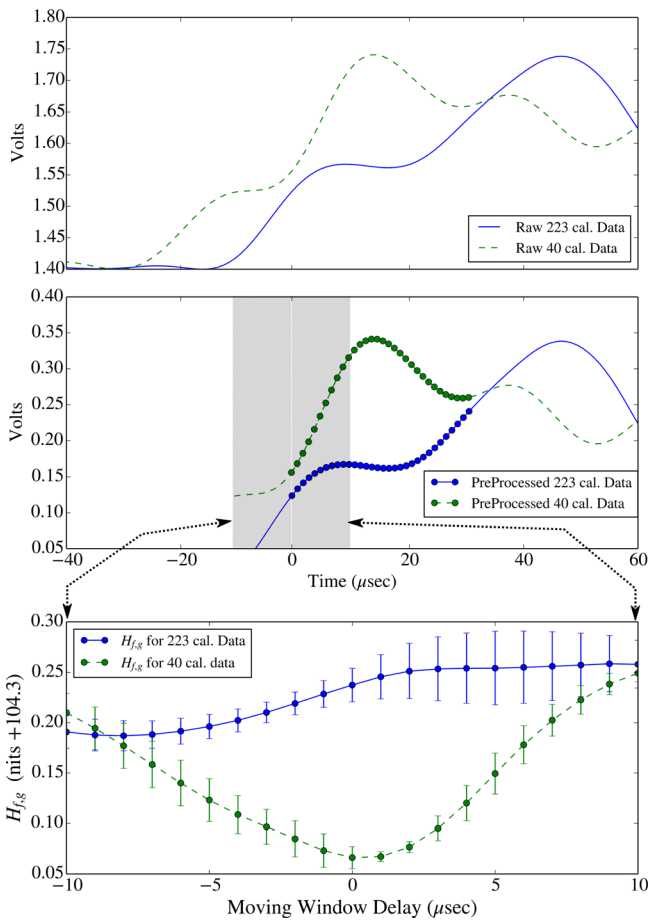

FIG. 6. (Color online) Effect of changing analysis parameters. Top panel: raw data for 223 caliber assault rifle and 40 caliber pistol. Middle panel: curves for bandpass filtered data with circular symbols indicating first set of points used for $H_{g,f}$ analysis results in Fig. 3. The gray region indicates the range of starting times used to prepare the bottom panel. Bottom panel: Effect of changing the starting time for the set of points used to compute $H_{f,g}$.

V. DISCUSSION

The results summarized in Tables II and III suggest that a statistical detection and identification system based on the complementary use of the logarithm of signal energy and the joint entropies [one for each reference function $g_i(t)$] could be developed that would simultaneously detect discharge of firearms and classify their type. This system could be based on a hierarchical analysis beginning with $\log[E_f]$ analysis to discriminate between threat and nonthreat events. If the former were indicated by the energy analysis then subsequent firearm identification would be executed using H_{f,g_i} signal receivers.

While the use of confidence ratios is a useful starting point for quantifying the statistical separation between random variables, the hierarchical analysis indicated above would require explicit knowledge of their distributions. Unfortunately, time and resource limitations precluded acquisition of a large number of firearm discharges of even a single weapon type.

Nevertheless, two conclusions seem warranted. First, and most important, is that for each firearm type there exists a receiver, either $\log[E_f]$ or one of the entropies H_{f,g_i}, that is tightly clustered with a large enough difference in mean values between different weapon types so that even a small sample of waveforms would be sufficient for statistical identification. In many cases, those where confidence ratios are larger than five, it appears that even a single weapon discharge would permit classification of a firearm into either the category of pistol or long rifle. The case where the standard deviation (σ) is less than five, identification and classification would still be possible since, unfortunately, multiple acoustic emissions from each firearm source would likely be available. In that case, statistical analysis could be based on the standard deviation of the mean ($\sigma/\sqrt{n}$), which decreases like $1/\sqrt{n}$ as the number, n of waveforms of each weapon type increases. For even a few discharges of each weapon type, $\sigma/\sqrt{n}$ would rapidly decrease so that the separations between accumulating mean values would approach five standard errors of the mean provided that the standard deviation exceeded one. To put these numbers in context suppose for the moment that the underlying distributions are normal. Then, taking the number of public elementary, middle, and high schools in the United States to be 100 000,[25] and assuming that each school has 1000 rooms and that there is an

acoustic event in each of these rooms once an hour for 24 h every day of the year, five sigma implies one false call will be made per century. While some of the numbers in this estimate may seem high, particularly the number of rooms per school, they have been chosen in order to provide an overestimate of the possible error rate.

Second, the expense of an expanded study to measure the distributions of $\log[E_f]$ and H_{f,g_i} is justified. The value of such an expanded study would lie in its use for design of an automated processing algorithm for detection of firearm discharges in public gathering places as well as the identification of firearm type.

ACKNOWLEDGMENTS

This study was funded by internal R&D funds at PNNL including the Signature Discovery Initiative. In addition, we would like to thank Steve Meyer, Special Response Team Commander, and Officers Barry Woodson and Steve Voit of the Hanford Patrol (U.S. Department of Energy) who assisted in acquisition of firearms data during the initial stages of this investigation. J.E.M. was partially supported by NSF grant DMS 1300280. M.S.H. and J.E.M. have a financial (ownership) interest in EntropyVision Inc. and may financially benefit if the company is successful in marketing its products that are related to this research.

APPENDIX

While it appears to be widely accepted that firearm discharges are capable of producing hearing loss, and thus exceed 140 dB levels required for this to occur, we have been unable to find refereed sources providing quantitative sound levels for specific measurement positions relative to the location of the firearm barrel. Several web sites contain data and plots, for instance: http://www.freehearingtest.com/hia_gunfirenoise.shtml or for more detailed description of actual measurements: Kyttala and Paakonen (1995): "Suppressors and shooting range structures" (http://www.guns.connect.fi/rs/suppress.html), which shows 160 dB maximum levels for a shooter firing a FN FAL L1A1 assault rifle using. 308 Win standard high velocity ammunition.

This matches the maximum safe operating level for the InvenSense INMP404ACEZ-R7 microphone used in our study, which indicates some risk in employing this device. Nevertheless, as our goal was demonstration of a low-cost, hence widely deployable, sensor we decided to proceed using the following precautions. First, rough amplitude comparisons of microphone output before and after a subset of the firearm discharges were performed using acoustic sources like the "wrench" and "book slap" to check for obvious changes in microphone output amplitude or shape. Second, the transducer was located at least 2 m from the acoustic source (firearm) during all testing, and probably experienced peak sound levels below 160 dB. Third, as it true for most engineering tolerances, the 160 dB safe operating level published by the manufacturer has probably been "de-rated" to provide an extra margin for safe use and is below the actual noise level at which the microphone suffers permanent damage. Fourth, and most important, quantitative comparisons of spectral characteristics of the microphone with unused microphones of the same manufacture could be performed at the conclusion of the study to rule out the possibility of microphone damage.

These quantitative comparisons were performed using four InvenSense INMP404ACEZ-R7 microphones that were not exposed to firearm discharges. The apparatus used to make these measurements is shown in Fig. 7. The speaker, a Sontron SPS-29-T00 piezo-ceramic with a 20 mm diameter, was used to drive the microphone under test. Given the constraints imposed by laboratory space and the desire to minimize cable lengths for the electronic components, it was placed 42.8 cm away from the microphone. This is greater than the near-to-far field transition point, for 26 kHz, which occurs at 6.1 cm.

In order to ensure measurement of all microphones occurred in their linear response regime, calibration curves were acquired by measuring spectra of received pulses obtained by driving the broadband-amplifier with a 2 μs step function pulse from the Tektronix AFG 3252C set to a height of either 1.5, 1.0. 0.5, 0.25, or 0.125 V. These measurements simultaneously verify the linearity of all components in the measurement chain: Tektronix AFG 3252C, HP 6327A, speaker and microphone. Typical curves, in this case the family obtained using the prototype microphone, are shown in Fig. 8. The top curve, labelled 1.25 V, is 3.5 dB above the calibration curve corresponding to an amplified 1.00 V step function excitation, as expected. The remaining curves are all 6 dB apart, also as expected. Since the 0.5 V labelled curve appears to be well within the linear range of the measurement apparatus this driving level was used for all spectral characterizations.

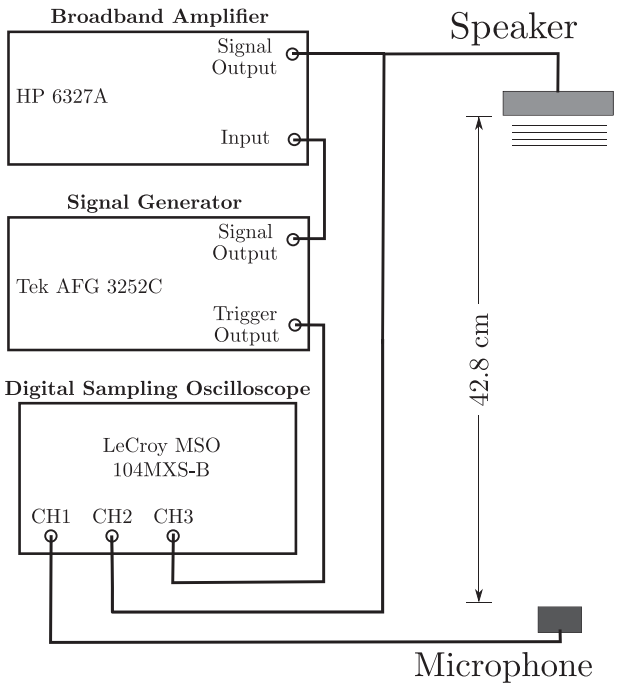

FIG. 7. Equipment diagram showing electronics used for measurements of spectral characteristics of InvenSense INMP404ACEZ-R7 microphones used in our study.

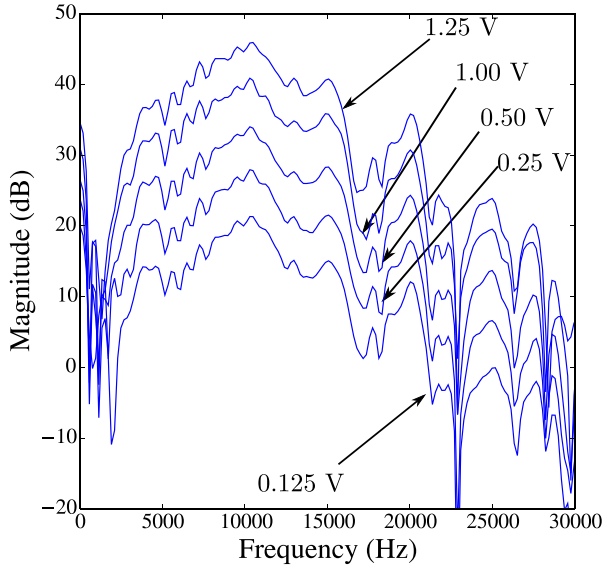

FIG. 8. (Color online) Typical calibration curves used to determine the amplitude of the square wave used for spectral measurements.

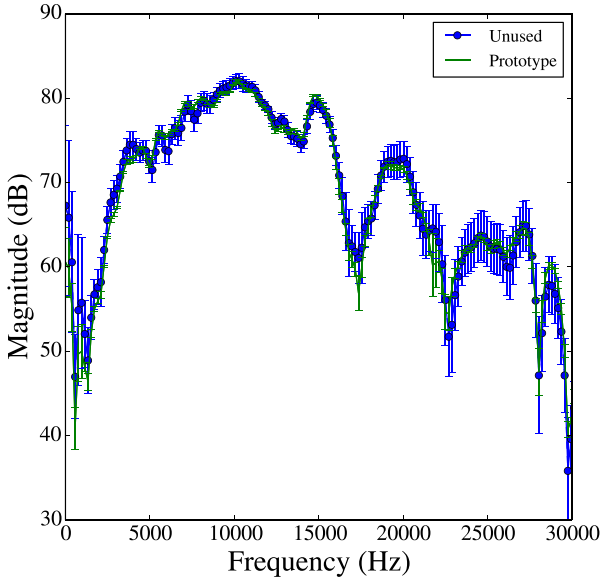

FIG. 9. (Color online) Comparison of spectra of prototype microphone after study completion with the average of five spectra obtained from unused microphone of the same manufacture. Standard deviation bars are also plotted.

Spectra were obtained using the following protocol. The prototype used to obtain firearm discharge data was placed in a clamp and aligned for maximum amplitude and arrival time of 1.25 ms (corresponding to 42.8 cm assuming a speed of sound of 343 m/s). The average of 256 pulses from the speaker were stored for later off-line analysis. Next, an unused microphone was placed in the clamp, its position and alignment similarly adjusted and the average of 256 pulses from the speaker were averaged and stored. This process was repeated for the remaining three unused microphones.

This cycle was repeated five times. Subsequently, the data were analyzed by baseline removal, windowing to eliminate spurious pulses and reduce noise using a 1 ms window. As the microphones exhibit variations in output amplitude, all pulses were then scaled to a maximum deviation, from DC, of one. This permits more precise comparison of the shapes of the spectra. Next, each of the rescaled pulses were Fourier transformed and their magnitudes as functions of frequency, i.e., the spectra, were computed. The five spectra from the prototype were averaged. Their standard deviations were also computed. The same processing was performed on each of the twenty pulses obtained from the unused microphones and these were averaged and the standard deviation computed. We point out that the rescaling performed in the time domain had the effect of reducing the resulting standard deviation of the ensemble of twenty spectra and thus produces a more stringent comparison between prototype and unused microphone spectra.

The comparison of average prototype and average unused microphone spectra over a range extending from 0 to 28.6 kHz is shown in Fig. 9. The averaged ($N = 5$) spectra for the prototype with standard deviation error bars are represented in the solid curve without plot symbols. The average ($N = 20$) spectra for the unused microphones are represented by the curve with circular symbols. The plots are essentially the same over the 1 to 26 kHz range used to bandpass filter all time domain data prior to the analysis that produced the comparisons shown in Figs. 3 and 5.

[1]M. Hughes, "Analysis of ultrasonic waveforms using Shannon entropy," Proc. - IEEE Ultrason. Symp. **2**, 1205–1209 (1992).
[2]M. Hughes, "Analysis of digitized waveforms using Shannon entropy," J. Acoust. Soc. Am. **93**(4), 892–906 (1993).
[3]M. Hughes, "NDE imaging of flaws using rapid computation of Shannon entropy," Proc. - IEEE Ultrason. Symp. **2**, 697–700 (1993).
[4]M. Hughes, "Analysis of digitized waveforms using Shannon entropy. II. High-speed algorithms based on Green's functions," J. Acoust. Soc. Am. **95**(5), 2582–2588 (1994).
[5]M. S. Hughes, J. N. Marsh, C. S. Hall, D. Savoy, M. J. Scott, J. S. Allen, E. K. Lacy, C. Carradine, G. M. Lanza, and S. A. Wickline, "Characterization of digital waveforms using thermodynamic analogs: Applications to detection of materials defects," IEEE Trans. Ultrason., Ferroelectr., Frequency Control **52**(9), 1555–1564 (2005).
[6]M. Hughes, J. McCarthy, J. Marsh, and S. Wickline, "Joint entropy of continuously differentiable ultrasonic waveforms," J. Acoust. Soc. Am. **133**(1), 283–300 (2013).
[7]M. Hughes, J. McCarthy, P. Bruillard, J. Marsh, and S. Wickline, "Entropic vs. energy waveform processing: A comparison based on the heat equation," Entropy **17**(6), 3518–3551 (2015).
[8]J. N. Marsh, J. E. McCarthy, M. Wickerhauser, J. M. Arbeit, R. W. Fuhrhop, K. D. Wallace, G. M. Lanza, S. A. Wickline, and M. S. Hughes, "Application of real-time calculation of a limiting form of the renyi entropy for molecular imaging of tumors," IEEE Trans. Ultrason., Ferroelectr. Frequency Control **57**(8), 1890–1895 (2010).
[9]J. N. Marsh, K. D. Wallace, G. M. Lanza, S. A. Wickline, M. S. Hughes, J. E. McCarthy, and M. V. Wickerhauser, "Application of a limiting form of the Renyi entropy for molecular imaging of tumors using a clinically relevant protocol," Proc. - IEEE Ultrason. Symp. **1**, 53–56 (2010).
[10]K. D. Wallace, J. Marsh, S. L. Baldwin, A. M. Connolly, K. Richard, G. M. Lanza, S. A. Wickline, and M. S. Hughes, "Sensitive ultrasonic delineation of steroid treatment in living dystrophic mice with energy-based and entropy-based radio frequency signal processing," IEEE Trans. Ultrason. Ferroelectr. Frequency Control **54**(11), 2291–2299 (2007).
[11]M. Hughes, J. Marsh, K. Wallace, T. Donahue, A. Connolly, G. M. Lanza, and S. A. Wickline, "Sensitive ultrasonic detection of dystrophic skeletal muscle in patients with Duchenne's muscular dystrophy using an entropy-based signal receiver," Ultrasound Med. Biol. **33**(8), 1236–1243 (2007).

[12]M. Hughes, J. Marsh, K. Agyem, J. McCarthy, B. Maurizi, M. Wickerhauser, K. Wallace, G. Lanza, and S. Wickline, "Use of smoothing splines for analysis of backscattered ultrasonic waveforms: Application to monitoring of steroid treatment of dystrophic mice," IEEE Trans. Ultrason. Ferroelectr. Frequency Control **58**(11), 2361–2369 (2011).
[13]R. Seip, E. Ebbini, and M. O'Donnell, "Non-invasive detection of thermal effects due to highly focused ultrasonic fields," Proc. - IEEE Ultrason. Symp. **2**, 1229–1232 (1993).
[14]R. Maher, "Acoustical characterization of gunshots," in *Signal Processing Applications for Public Security and Forensics, 2007. SAFE'07. IEEE Workshop on, Signal Processing Applications for Public Security and Forensics* (IEEE, Hoboken, NJ, 2007), pp. 1–5.
[15]P. Sinha, S. Kumar, and R. Hegde, "Sniper localization using passive acoustic measurements over an ad-hoc sensor array," in *2015 Twenty First National Conference on Communications (NCC)* (IEEE, Hoboken, NJ, 2015), pp. 1–6.
[16]M. Khalid, M. Babar, M. Zafar, and M. Zuhairi, "Gunshot detection and localization using sensor networks," in *2013 IEEE International Conference on Smart Instrumentation, Measurement and Applications (ICSIMA)* (IEEE, Hoboken, NJ, 2013).
[17]R. Maher, "Audio forensic examination," IEEE Signal Process. Mag. **26**(2), 84–94 (2009).
[18]A. Ramos, S. Holm, S. Gudvangen, and R. Otterlei, "A modified spectral subtraction algorithm for real-time noise reduction applied to gunshot acoustics," in *2012 International Conference on Signals and Electronic Systems (ICSES)* (IEEE, Hoboken, NJ, 2012), pp. 1–5.
[19]T. Ahmed, M. Uppal, and A. Muhammad, "Improving efficiency and reliability of gunshot detection systems," in *2013 IEEE International Conference on Acoustics, Speech and Signal Processing (ICASSP)* (IEEE, Hoboken, NJ, 2013), pp. 513–517.
[20]A. Chacn-Rodrguez, P. Julin, L. Castro, P. Alvarad, and N. Hernndez, "Evaluation of gunshot detection algorithms," IEEE Trans. Circuits Syst. **58**(2), 363–373 (2011).
[21]H. Zhao and H. Malik, "Audio recording location identification using acoustic environment signature," IEEE Trans. Inf. Forensics Secur. **8**(11), 1746–1759 (2013).
[22]P. Bevington, *Data Reduction and Error Analysis for the Physical Sciences*, 1st ed. (McGraw-Hill, New York, 1969), pp. 1–336.
[23]D. L. Sackett, "Why randomized controlled trials fail but needn't: 2. Failure to employ physiological statistics, or the only formula a clinician-trialist is ever likely to need (or understand!)," Can. Med. Assoc. J. **165**(9), 1226–1237 (2001).
[24]M. Hughes, J. McCarthy, P. Bruillard, J. Marsh, and S. Wickline, "Entropic vs. energy waveform processing: A comparison based on the heat equation," in *Proceedings of the Fall 2014 Acoustical Society Meeting* (ASA, Melville, NY, 2014).
[25]National Center for Education Statistics, Digest of Education Statistics (U. S. Department of Education, Alexandria, VA, 2015), Chap. 2.